J Solid State Eletrochem (2004) 8: 474–481
DOI 10.1007/s10008-003-0466-9

ORIGINAL PAPER

**Hainer Wackerbarth · Rodolphe Marie
Mikala Grubb · Jingdong Zhang · Allan G. Hansen
Ib Chorkendorff · Claus B. V. Christensen
Anja Boisen · Jens Ulstrup**

Thiol- and disulfide-modified oligonucleotide monolayer structures on polycrystalline and single-crystal Au(111) surfaces

Received: 4 July 2003 / Accepted: 1 October 2003 / Published online: 24 January 2004

Abstract We provide a comprehensive study of single- (ss) and double-strand (ds) oligonucleotides with either 25 or 10 bases or base pairs (bp) immobilized on polycrystalline and single-crystal Au(111) surfaces. The study is based on X-ray photoelectron spectroscopy, cyclic and differential pulse voltammetry, interfacial capacitance data, and electrochemical scanning tunnelling microscopy (in situ STM). The sequences used were the 25-bp sequence from the BRCA1 gene (25-mer), while the 10-bp oligonucleotides contained solely linear adenine and thymine sequences. The oligonucleotides were modified by the dimethoxytrityl group (DMT) via a disulfide group [DMT-S-S-ss25-mer and DMT-S-S-ds$(AT)_{10}$], a pure disulfide group (A_{10}-S-S-T_{10}), or a thiol group [HS-ss25-mer and HS-ds-$(AT)_{10}$], all via a hexamethylene linker. The overall pattern suggests strategies for controlled adsorption of DNA-based molecules and recognition of complementary strands or other molecules.

Keywords Adsorption · Electrochemistry · Oligonucleotides · Scanning tunnelling microscopy · X-ray photoelectron spectroscopy

H. Wackerbarth · M. Grubb · J. Zhang
A. G. Hansen · J. Ulstrup (✉)
Department of Chemistry, Building 207,
Technical University of Denmark,
2800 Lyngby, Denmark
E-mail: ju@kemi.dtu.dk
Tel.: +45-45252359
Fax: +45-45883136

R. Marie · C. B. V. Christensen · A. Boisen
Institute of Micro- and Nanotechnology,
Building 345 East, Technical University of Denmark,
2800 Lyngby, Denmark

I. Chorkendorff
Department of Physics and Department of Chemical Engineering,
ICAT (Interdisciplinary Research Center for Catalysis),
Technical University of Denmark, Building 309-312,
2800 Lyngby, Denmark

Introduction

Hybridization, electron transfer, and other functional properties of DNA-based molecules are crucial in DNA-based biotechnology towards the nanoscale and single-molecule levels [1, 2, 3, 4]. Rational approaches to nanoscale DNA-based "chips" and other biotechnology requires, however, that functional DNA-based molecules are immobilized in controlled adsorption modes on well-characterized, solid metallic or non-metallic surfaces. This implies, for example, that precisely defined atomic sites of the target molecules are linked to the surface. The spacing between the immobilized target molecules must also be controlled to an extent that proteins or complementary DNA-based partners can be recognized by the immobilized target molecules. Variation of controlling external parameters for the adsorption is, finally, a desirable nanoscale biotechnological feature. Electrostatic control of the orientation of the adsorbed strongly negatively charged poly-anionic single- or double-strand probe molecules by variation of the electrochemical potential of metallic substrates is here an immediate option. This holds the further merits of environmental control directly in the aqueous buffer media needed for biotechnological DNA-based molecular function. Control of these adsorption features would clearly extend the perspectives for real nanoscale biotechnology towards the single-molecule level. This would include imaging of single-molecule functional chemical events and, on longer terms, enable better assessment of other "DNA-chip"-based potential in the contexts of nanoscale and molecular electronic circuit components [5, 6, 7, 8, 9, 10, 11, 12].

In this report we provide comprehensive data for the adsorption dynamics of several functionalized single- and double-strand oligonucleotides on polycrystalline and single-crystal Au(111) surfaces. Two classes of target molecules have been chosen. One is a single-strand 25-base probe from the breast cancer susceptibility gene (BRCA1). This molecule has an immediate conspicuous

importance in the diagnostics of inherited susceptibility to breast cancer [13]. The other class is based on shorter single- and double-strand oligonucleotides of simple base composition, i.e. sequences composed solely of 10 adenines or thymines [14]. The deca-nucleotides are long enough to display collective two-dimensional properties in the adsorbed state but short enough that imaging by scanning tunnelling microscopy (STM) based on electron tunnelling through the adsorbed molecules can be envisaged. The oligonucleotides have been functionalized by thiol or disulfide groups suitable for gentle linking to polycrystalline or single-crystal Au(111) surfaces. The data are based on X-ray photoelectron spectroscopy (XPS), voltammetric and other electrochemical data, and on electrochemical scanning tunnelling microscopy directly in aqueous buffer (in situ STM). The data have disclosed a detailed view of the variable adsorption modes of these differently modified, technologically relevant DNA-based molecules on polycrystalline and single-crystal Au(111) surfaces. They also offer suggestions as to strategic principles for single-molecule DNA-based chemical and biological "sensors" and "chips".

Experimental

Reagents

All oligonucleotides were synthesized by TAG Copenhagen (Denmark). Double-stranded 10-mer oligonucleotides modified with a disulfide bridge and a dimethoxytrityl (DMT) group are referred to as DMT-S-S-ds$(AT)_{10}$, double-stranded 10-mer oligonucleotide modified with a disulfide bridge or a thiol linker as A_{10}-S-S-T_{10} and HS-ds-$(AT)_{10}$, respectively (Fig. 1). The sequence of the 25-mer single-stranded probe from the BRCA1 gene used in this study is 5′-ATT AAT GCT ATG CAG AAA ATC TTA G-3′. The unmodified single-stranded 25-mer oligonucleotide is referred to as ss25-mer. The single- and double-stranded 25-mer modified with a mercaptohexyl group at the 5′-end are denoted as HS-ss25-mer and HS-ds25-mer, respectively. A single-stranded 25-mer modified with a DMT group and a disulfide bridge, in short DMT-S-S-ss25-mer, was also used. If specified, the DMT-S-S-ss25-mer was subjected to the de-protection protocol from Glen Research (USA), whereby the molecule was de-protected to HS-ss25-mer using DTT in TEAA buffer. The resulting HS-ss25-mer was diluted in water to the desired concentration.

KH_2PO_4 and K_2HPO_4 buffers were suprapure grade. All other chemicals were analytical grade. MilliQ water (Milli-Q Housing, 18.2 MΩ) was used throughout. Hydrogen peroxide, hydrochloric acid, nitric acid, sulfuric acid, acetone, dithiothreitol (DTT), and 1-mercapto-6-hexanol (MCH) were from Sigma (Sternheim, Germany); triethylammonium acetate (TEAA) was from Fluka (Buchs, Switzerland); and silver nitrate and ethanol were from Allied Signal (Riedel-de Haën, Germany).

Sample preparation

Polycrystalline gold layers

The substrates were standard silicon wafers with a 1000 Å top silicon nitride layer on which 100 Å chromium and 600 Å gold layers were evaporated 72 h prior to the deposition of the molecules. The substrates were cleaned in 33% aqua regia (1 part HNO_3 plus 3 parts HCl) for 30 s and stored in water until adsorption of the molecules.

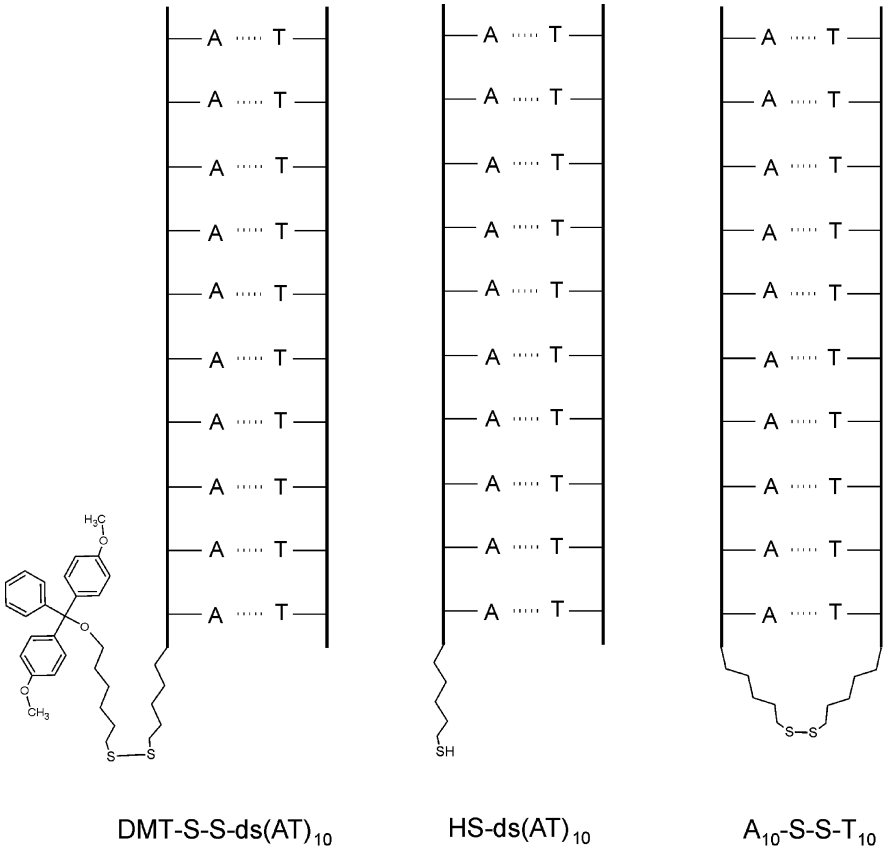

Fig. 1 Schematic illustration of the thiol modifications of the double-stranded oligonucleotides

Single-crystal gold electrodes

Single-crystal gold electrodes for electrochemistry were prepared as bead electrodes by the method of Clavilier and Hamelin [15, 16] or acquired from Surface Preparation Laboratory (The Netherlands). A Au(111) disc (Surface Preparation Laboratory, 10 mm diameter and 1 mm thick) was used as substrate in STM and XPS studies. The bead electrodes and substrate were electropolished in 0.1 M H_2SO_4 (10 V, followed by soaking in 1 M HCl) and annealed in an oven at 850 °C for 5 h. Prior to use the disc or bead electrodes were annealed for 2 min in a hydrogen flame. The disc substrates were cooled to room temperature in air. The bead electrodes were cooled above a Millipore water surface, followed by immersion in the water. The substrate or electrode was, finally, transferred to an aqueous solution of oligonucleotides in 1 M phosphate buffer.

The quality of all single-crystal gold electrodes was checked on a regular basis by recording cyclic voltammograms in 0.1 M H_2SO_4. Agreement with reported voltammograms at Au(111) electrode surfaces was taken as a satisfactory quality check [16].

Sample preparation for X-ray photoelectron spectroscopy

The 25-mer single-stranded DNA probes in the protected form (DMT-S-S-ss25-mer) were used on polycrystalline gold. Three oligonucleotide samples and two gold references were prepared. The HS-ss25-mer was adsorbed for 10 min from a 300 μM solution of oligonucleotide, de-protected according to the protocol above. The surface was then washed in water for 10 min in order to remove weakly bound adsorbate molecules. The DMT-S-S-ss25-mer was adsorbed at a concentration of 300 μM and washed in water for 10 min. The last sample was exposed to a 300 μM solution of DMT-S-S-ss25-mer and left to dry on the surface, resulting in an adsorbate multi-layer. In addition, two reference gold surfaces were prepared. Reference 1 was an as-deposited gold surface; reference 2 was a gold surface cleaned for 30 min in aqua regia.

Three Au(111) samples were prepared for XPS. In one sample, MCH dissolved in H_2O (1 mM) was brought to adsorb for several hours at room temperature. DMT-S-S-ds$(AT)_{10}$ (1 μM) was adsorbed for 18 h at 5 °C to prepare the second sample. In the third sample, A_{10}-S-S-T_{10} (1 μM) was adsorbed for 42 h at room temperature. All samples were subsequently thoroughly rinsed with Millipore water.

Instrumentation

X-ray photoelectron spectroscopy

The XPS analysis was performed on a Perkin-Elmer Instrument model 550 ESCA/SAM (1 eV resolution at a pass energy of 50 eV) with a double-pass cylindrical-mirror analyzer equipped for angle-resolved measurements. The work function of the detector, ϕ_s, was 5.4 eV. A monochromatic magnesium X-ray source (1253.6 eV, corresponding to the Kα transition energy of Mg) was used for excitation and the photoelectrons collected at 42.3° from the surface normal. Survey spectra were recorded from 0 to 1000 eV in steps of 1 eV with a pass energy of 50 eV and a speed of 500 ms/step, and 180° angular position of the aperture (normal exit angle). Detailed spectra were recorded from 156 to 170 eV in steps of 1 eV with a pass energy of 25 eV and a speed of 500 ms/step, and 0° angular position of the aperture (grazing exit angle).

Spectral deconvolution of the sulfur emission band was performed using least-squares fitting of a doublet of Gaussian profiles from the $2p_{1/2}$ and $2p_{3/2}$ emission bands [denoted as S($2p_{1/2}$) and S($2p_{3/2}$)] and a linear base line function [17]. For every doublet the amplitude ratio of the two Gaussian profiles is 1:2 [S($2p_{1/2}$):S($2p_{3/2}$)] and the splitting energy 1.2 eV [18]. For deconvolutions involving more than one doublet, amplitudes and binding energies are used as fitting parameters, while the peak width is taken to be the same for every doublet.

Voltammetry and capacitance measurements

Only bead electrodes were used for interfacial capacitance data, cyclic (CV) and differential pulse voltammetry (DPV). Glassware and other utensils were cleaned as previously described [19]. The hanging meniscus method was used. CV, DPV, and interfacial capacitances were recorded using an Autolab system (Eco Chemie, The Netherlands) controlled by GPES software. Parameters in DPV and capacitance measurements were a 10 mV s^{-1} scan rate and a 4.05 mV step potential in DPV, 100 Hz and 5 mV modulation amplitude in capacitance measurements [19, 20]. A coiled bright platinum wire and a saturated calomel electrode (SCE) were used as counter and reference electrodes, respectively. All potentials refer to SCE. A 0.1 M K_2HPO_4/KH_2PO_4 buffer (pH 6.9) was the medium for the electrochemical measurements. The solutions were deoxygenated by bubbling purified argon (Chrompack, 5N) through the solution prior to use and an argon atmosphere maintained above the solutions during experimental recordings.

In situ STM

A PicoSPM instrument (Molecular Imaging, USA), with a bipotentiostat for independent control of substrate and tip potential, and in-house-built three-electrode KEL-F cells were used in the constant current mode. The substrate was a Au(111) disc (cf. above). Reference and counter electrodes were platinum wires. The supporting electrolyte was 0.01 M phosphate (ca. pH 7). Tungsten tips were prepared and coated as previously described [21].

Results

XPS was used to investigate the nature of the sulfur bond between the thiol-modified oligonucleotides and the gold substrate. XPS of HS-ss25-mer, DMT-S-S-ss25-mer, and DMT-S-S-ss25-mer with an increased layer thickness was based on polycrystalline gold, with two bare reference polycrystalline gold surfaces. XPS of MCH, DMT-S-S-ds$(AT)_{10}$, and the disulfide complementary 10-mer A_{10}-S-S-T_{10} was based on Au(111). Carbon (C 1s, 284.6 eV), oxygen (O 1s, 531.6 eV), and nitrogen (N 1s, 400 eV) were identified on the survey spectra of all samples. The low signal for nitrogen compared to the Au $4f_{7/2}$ line on references 1 and 2 indicates a low contamination of the gold surface. The high ratios for sample 3 indicates that the adsorbate layer is considerably thicker on sample 3 than on the other five samples.

The binding state of the sulfur atoms is determined from the detailed spectra. On polycrystalline gold, one doublet of Gaussian profiles is sufficient for deconvoluting the HS-ss25-mer spectrum (Fig. 2A). The S($2p_{3/2}$) binding energy is 162.2 eV and the peak width 1.03 eV. These two parameters are conserved in the spectra of DMT-S-S-ss25-mer and the thick layer of DMT-S-S-ss25-mer. The sulfur emission band is, however, broader for DMT-S-S-ss25-mer (Fig. 2B). A second doublet was therefore introduced with a S($2p_{3/2}$) binding energy of 163.9 eV. The detailed spectrum of the thick layer of DMT-S-S-ss25-mer is shown in Fig. 2C. The sulfur peak is obviously shifted toward higher binding energy. A third doublet is therefore introduced in this spectrum. The S($2p_{3/2}$) binding energy of the new doublet is

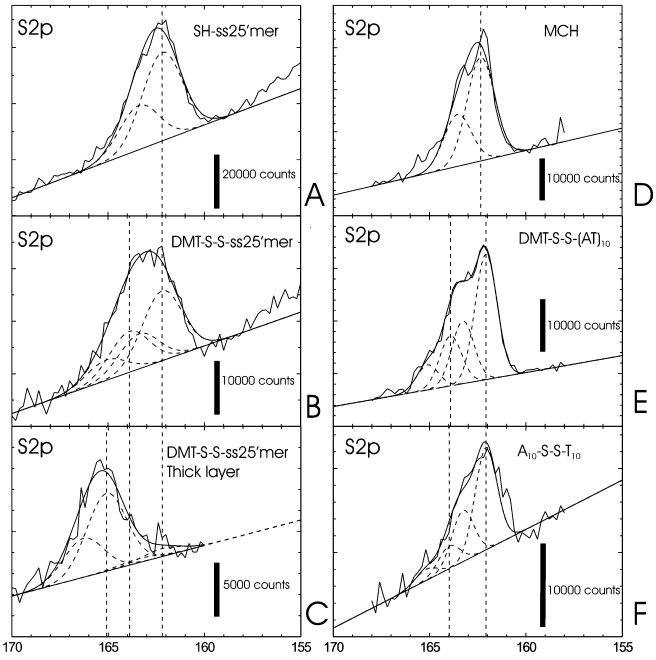

Fig. 2 Detailed XPS spectra of the polycrystalline (*left*) and single-crystal (*right*) samples in the S 2p region. The fitting curves and the base lines appear as *fully drawn lines* and the Gaussian doublets as *dashed lines*. The *vertical dashed lines* indicate the $S(2p_{3/2})$ binding energies of the doublets used in the fitting procedure

165.1 eV, with an amplitude 10-fold higher than for the other two doublets. A single doublet with a binding energy of 162.3 eV and a width of 0.71 eV is sufficient to fit the spectrum of MCH on Au(111) (Fig. 2D). As shown in Fig. 2E and Fig. 2F, the spectra of DMT-S-S-ds$(AT)_{10}$ and A_{10}-S-S-T_{10} are broader and therefore deconvoluted, with two doublets with the same binding energies (162.1 and 163.9 eV) and width (0.56 eV) for both samples. The binding energies, full width at half maximum, and the amount of doublets are listed in Table 1.

The binding energy value of 162.2 ± 0.1 eV obtained for HS-ss25-mer, MCH, and used in the deconvolution of the spectra of DMT-S-S-ss25-mer, DMT-S-S-$(AT)_{10}$, and A_{10}-S-S-T_{10} is in good agreement with the value of 162.0 eV reported for alkanethiols on gold [18]. A comparison of the amplitudes of the two doublets in Fig. 2 (B, E and F) suggests that 38, 18 and 28%, respectively, of the protected oligonucleotides are non-specifically adsorbed to the gold surface.

Electrochemistry is a powerful tool for analyzing other physical properties of adlayers. Figure 3 shows cyclic voltammograms and interfacial capacitance data for HS-ds-25-mer on Au(111) in 100 mM phosphate, pH 7. Voltammetric scans to negative potentials reduce the Au–S bond, liberating the thiol-containing molecules. Reductive desorption is usually performed in basic solution to avoid electrochemical dihydrogen evolution. This interference was of minor importance in the present study. Reductive desorption is a valuable method to determine the surface coverage, inasmuch as one electron is consumed for each reductively desorbed molecule. Figure 3A shows three subsequent cyclic voltammetric scans. A peak at −675 mV appears in the first scan but decays in the following scans, supporting that the covalently attached HS-ds-25-mer is reductively desorbed with no re-adsorption. Analogous behavior was observed for the single-strand HS-ss-25-mer The calculated charge is 10.7 $\mu C/cm^{-2}$. The results of cyclic voltammetry for the thiolated double- and single-stranded oligomers are summarized in Table 2.

The adsorption of the oligonucleotides is also reflected in the interfacial capacitance. The first scan (a) in

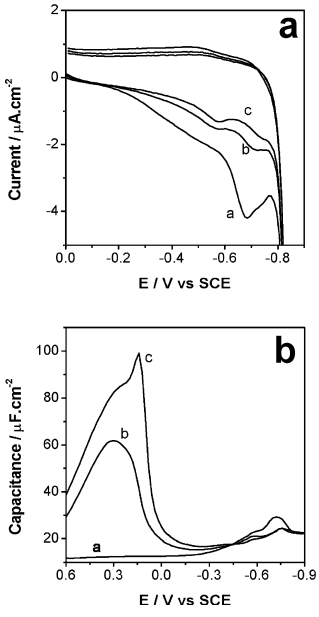

Fig. 3 Cyclic voltammograms (**a**) and interfacial capacitance (**b**) of the mercaptohexyl ds-25-mer on Au(111); 100 mM phoshate buffer, pH 6.9. (*a*) First scan, (*b*) second scan, and (*c*) third scan. Scan rate in **a**: 10 mV s^{-1}

Table 1 Parameters of the fitted XPS spectra of thiol-modified oligonucleotides and MCH

Sample	B.e.,[a] first doublet (eV)	FWHM(eV)[b]	B.e.,[a] second doublet (eV)	B.e.,[a] third doublet (eV)
HS-ss25-mer	162.19	1.03		
DMT-S-S-ss25-mer	162.19	1.03	163.88	
DMT-S-S-ss25-mer	162.19	1.03	163.88	165.05
MCH	162.34	0.71		
DMT-S-S-ds$(AT)_{10}$	162.07	0.56	163.91	
A_{10}-S-S-T_{10}	162.07	0.56	163.98	

[a]Binding energy of $S(2p_{3/2})$
[b]Full width at half maximum

Table 2 Reductive desorption of thiolated oligonucleotides

Sample	Peak (mV)	CV charge ($\mu C\ cm^{-2}$)	Capacitance charge ($\mu C\ cm^{-2}$)	Coverage (pmol cm^{-2})
HS-ss-25-mer	-733 ± 34	26.9 ± 4	2.2	260 ± 40
HS-ds-25-mer	-685 ± 7	9.9 ± 1	1.7	80 ± 10

Fig. 3B shows a nearly constant capacitance of around 12 μFcm^{-2} between 0.6 and −0.15 V and a peak at −0.72 V with a shoulder on the high-potential side. The figure also shows the interfacial capacitance after one (b) and two (c) negative potential excursions beyond the reductive desorption potential. These scans show a large hump around the potential of zero charge, caused by increasing adsorption of mono- and dihydrogen phosphate ions. Scan (c) in fact closely resembles the interfacial capacitance of pure phosphate buffer solution on Au(111) with a typical sharp peak at 0.15 V, reflecting lifting of the Au(111) surface reconstruction.

Figure 4 shows differential pulse voltammograms (DPVs) of the thiolated and thiol-free single-stranded oligonucleotides. The DPV of HS-ss-25-mer shows a peak around −710 mV. Although the ss-25-mer is not attached to the Au(111) surface via sulfur, the voltammogram of the thiol-free ss-25-mer also shows a peak around −720 mV, but the peak size is significantly smaller compared to the thiolated oligonucleotides. Moreover, there are two additional peaks, which are not present for the thiol-modified 25-mer.

Figure 5 shows the interfacial capacitance of HS-ds-25-mer (a), HS-ss-25-mer (b), and ss-25-mer (c). The mercaptohexyl-modified 25-mers show a featureless background and both have a pronounced peak at −720 mV with a shoulder towards positive potentials. The unmodified ss-25-mer shows some features and three smaller peaks at −520, −720, and −850 mV. The interfacial capacitance between 0.6 and −0.15 V is higher for HS-ss-25-mer than for HS-ds-25-mer, indicating a difference in the layer properties, which can be interpreted as a lower permeability and hence a closer packing [22].

Figure 6 shows, finally, an in situ STM image of the protected-ds-$(AT)_{10}$. The size of the white spots accords with the dimensions of the single oligonucleotide molecules. The white spots cover about 23% of the surface. In contrast, the image of the disulfide-ds-$(AT)_{10}$ in Fig. 7 has a completely different character. Single molecules can no longer be resolved, but the black spots or pits, typical for alkanethiol layers, indicate that a high density of oligonucleotides is present on the surface.

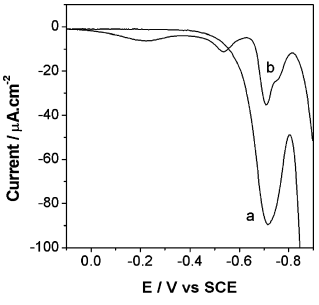

Fig. 4 Differential pulse voltammograms of mercaptohexyl ss-25-mer (*a*) and ss-25-mer (*b*) on Au(111); 100 mM phosphate buffer, pH 6.9. Step potential: 4.05 mV; modulation amplitude: 25.05 mV; scan rate: 10 mV s^{-1}

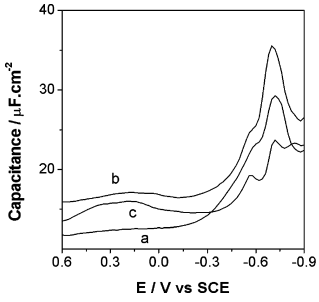

Fig. 5 Interfacial capacitance of mercaptohexyl ds-25-mer (*a*), mercaptohexyl ss-25-mer (*b*), and ss-25-mer (*c*) on Au(111); 100 mM phosphate buffer, pH 6.9

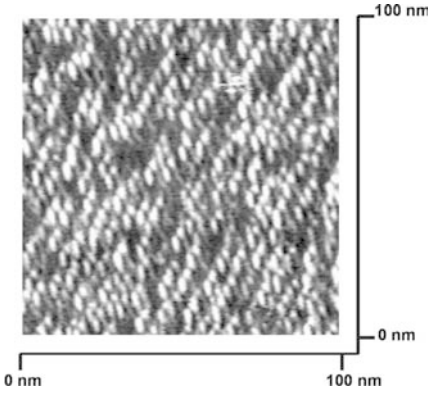

Fig. 6 In situ STM image of DMT-S-S-ds$(AT)_{10}$ adsorbed on Au(111) in 10 mM phosphate buffer, pH 6.8. Constant-current mode; area: 100 nm×100 nm; tunnel current: 0.12 nA; sample potential: −0.21 V; bias voltage: −0.15 V; scan rate: 13 lines s^{-1}

Discussion

Binding states of protected and de-protected oligonucleotide layers

The XPS data show clearly that all the thiol- and disulfide-modified oligonucleotides are specifically adsorbed on polycrystalline gold or single-crystal Au(111) via the sulfur atom(s). The spectral resolution of HS-

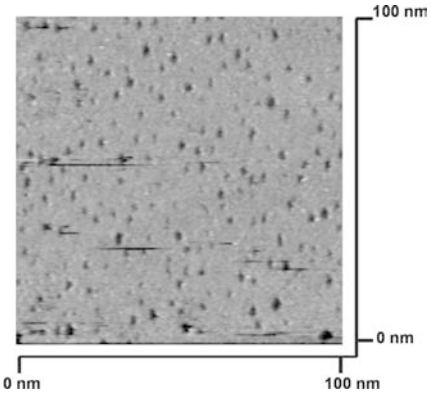

Fig. 7 In situ STM image of A_{10}-S-S-T_{10} adsorbed on Au(111); 10 mM phosphate buffer, pH 6.8. Constant-current mode; area: 100 nm×100 nm; tunnel current: 0.1 nA; sample potential: −0.66 V; bias voltage: −0.2 V; scan rate: 9.8 lines s^{-1}

ss25-mer and MCH suggests that the sulfur atoms on the polycrystalline Au surface and single-crystal Au(111) surface, respectively, are present in a single chemisorbed state. The higher binding energy of 165.1 eV for the thick DMT-SS-ssDNA layer compared to the HS-ss25-mer and MCH is indicative of less metallic screening. This can be associated with sulfur atoms in a disulfide bridge not interacting with the gold surface. A third doublet was introduced in the spectra of the DMT-S-S-ss25-mer, DMT-S-S-$(AT)_{10}$, and A_{10}-S-S-T_{10}. The energy of this doublet is consistently 163.9 ± 0.1 eV. This new binding energy suggests that sulfur is also present in a third chemical state. This state exhibits a lower binding energy than the bridged sulfur in the DMT-S-S-ss25-mer, but a higher energy than for sulfur chemisorbed on gold (HS-ss25-mer and MCH). These sulfur atoms are believed to be present on the gold surface in both bridged and physisorbed state. The proximity of the gold surface induces electrostatic screening which lowers the binding energy, but the electrostatic screening is not as efficient as for the direct binding of sulfur to the gold surface. This is also consistent with the fact that this type of sulfur atom is present only for the molecules with a disulfide bridge and not for the HS-ss25-mer.

Three different adsorption states of the modified oligonucleotide molecules both on polycrystalline and single-crystalline gold were thus observed by XPS both on polycrystalline and single-crystalline gold. HS-ss25-mer and MCH only display direct chemisorption of sulfur, whereas molecules containing a disulfide bridge exhibit both chemisorption of sulfur and physisorption of the sulfur bridges. Finally, the thick layer of DMT-S-S-ss25-mer seems to display an additional signal from free sulfur bridges. These combined observations offer clues to the chemical pathway for chemisorption of the protected oligonucleotides to gold. As expected from the earlier study of heterodimers of alkanethiols on gold, the protected oligonucleotides are probably first adsorbed non-specifically on gold via the disulfide bridges. The disulfide bridge then breaks in some of the molecules and the liberated sulfur atoms bind to the gold surface, leading to chemisorption of the oligonucleotides [23].

Coverage and voltammetric behavior of the thiolated oligonucleotide layers

The voltammograms and interfacial capacitance of the thiol-modified and unmodified oligonucleotides point towards substantially different adsorption modes. DNA is a polyelectrolyte. The backbone is strongly negatively charged at neutral pH, whereas the nitrogen-containing side chains are positively charged. The adsorption mode of thiol-free DNA therefore depends on the polarization of the surface. Changes in the adsorption mode, possibly involving protonation and deprotonation of the oligonucleotides and finally desorption, cause non-Faradaic, capacitive currents. This may be the origin of the DPV and interfacial capacitance peaks, inasmuch as DNA desorbs from polycrystalline gold at −0.8 V before reduction takes place. Moreover, the interfacial capacitance of the ss-25-mer resembles that of denaturated DNA on polycrystalline gold [24]. In contrast to native double-strand DNA, single-strand and denaturated DNA can interact directly via the nucleobases with the surface. The interplay between collective properties and the complex potential-dependent adsorption/reorientation behavior found for single nucleobases and nucleosides on gold does not admit a further interpretation of the data [25, 26, 27, 28, 29]. Oligonucleotides containing only one type of nucleobases combined with single-crystal electrochemistry and in situ STM are certainly a promising approach in this context.

The open circuit potential of the Au(111) electrode in 0.1 M phosphate buffer (0.19 V) indicates that the surface is negatively polarized during the adsorption process. This supports the formation of the gold–sulfur bond of the thiol-modified oligonucleotides, as the prevailing negatively charged backbone would be repelled from the negatively polarized surface. An adsorption mode is therefore favored, where sulfur binds to the gold surface and the oligonucleotide towards the solution. In contrast, the linker-free oligonucleotides would lie flat on the surface. In an adsorption mode where oligonucleotide binding is mainly via the thiol linker, the peak around −0.7 V stems primarily from reductive desorption of the thiol-linked oligonucleotide. This is strongly supported by the XPS results of the HS-ss-25mer. The charge of the peak can thus be directly used to determine the coverage on Au(111) surface. However, part of the charge still originates from a capacitive component caused by the formation of the aqueous double layer on the uncoated gold surface after thiolated oligonucleotide desorption. The interfacial capacitance data suggest that these contributions are 8% and 18% of the whole charge for the HS-ss-25-mer and the HS-ds-25-mer, respectively. These values are reasonable, compared with the capacitive component of alkanethiols [30, 31,

32], but represent an upper limit, inasmuch as the measured interfacial capacitance includes an Ohmic resistance, which cannot be separated by pure interfacial capacitance measurements. Subtracting the capacitive charges results in coverages of 260 and 80 pmol cm^{-2} for the HS-ss-25-mer and the HS-ds-25-mer, respectively.

Recumbent or flat-lying single- and double-stranded oligonucleotides with 25 bases should have a coverage about 20 and 10 pmol cm^{-2}, respectively. Zhang et al. [33] found a coverage of 7.5 pmol cm^{-2} for a double-stranded 30-mer containing solely adenine and thymine. The significantly higher coverage presented in this work therefore points to a non-recumbent adsorption mode. A simple estimate shows that single-stranded oligonucleotides in an upright position give a coverage about 210 pmol cm^{-2}, assuming a cylindrical geometry with a diameter of 10 Å. This is in agreement with the experiments. In an upright or tilted position, the coverage would, moreover, be little affected by the number of bases defining the length. The almost identical charges for thiolated single-stranded oligonucleotide containing 10 adenines (260 pmol cm^{-2}) and the HS-ss-25-mer therefore substantiate an upright or tilted position of the adsorbates [34]. In addition, hybridization of the oligonucleotide doubles the diameter and thus affects the coverage significantly. The coverage decreases to 80 pmol cm^{-2}. This agrees well with a coverage of 60–75 pmol cm^{-2} observed by O'Kelley et al. [6].

The position of the reductive desorption peak reflects the properties of the adlayer, i.e. solubility, lateral interactions, packing density, etc. However, the difference in the peak position of the cyclic voltammograms should not be overvalued, because of the broadness of the peaks which possibly reflects the coexistence of different adsorption modes.

Topographical information about the thiolated oligonucleotide layers

In situ STM images of protected DMT-S-S-ds$(AT)_{10}$ show clearly single-molecule features. XPS of this molecule clearly indicates that most of the disulfide bonds break on the surface and gold–sulfur bonds are formed. This implies that the protection group and the thiolated oligonucleotide both bind to the surface, and hence a mixed monolayer is present on the surface. Interactions between adjacent oligonucleotides are then hampered by steric hindrance, caused by the bulky protection group. In contrast, the disulfide A_{10}-S-S-T_{10} shows an unresolved dense monolayer, indicative of strong interactions between neighboring oligonucleotides. The in situ STM image of DMT-S-S-ds$(AT)_{10}$ does not answer the question of whether the oligonucleotides are adsorbed in a recumbent or an upright position. The oligonucleotides are quite flexible, because of the absence of stabilizing interactions, and the STM tip can cause bending of the oligonucleotides. The resolution is not sufficient to disentangle the tilt angle between the surface and the oligonucleotide.

In contrast, A_{10}-S-S-T_{10} self-assembles densely, in accordance with cyclic voltammetry of the 25-mer. Unhindered attractive lateral interactions between the adsorbed oligonucleotides are therefore likely, but must involve positive counter ions. From a biotechnological point of view, dense packing is unfavorable because of the blocked accessibility of the template-assembled DNA-based molecules. Accessibility is essential for DNA-based molecular devices, hybridization, and other biological screening. Adsorption of the protected oligonucleotides therefore offers an attractive approach to prepare functional template-based DNA monolayers. The spacer function of the protection group can thus be instrumentalized as a sensor in biotechnological screening. Surface coverage regulation of thiol-derivatized DNA-based molecules by formation of mixed oligonucleotide/spacer molecule monolayers on the surface is another way of controlling the accessibility of the DNA-based molecules used by Herne et al. [35].

Conclusions

XPS of disulfide- and thiol-modified oligonucleotides points to different adsorption modes. The HS-ss25-mer was well represented by a single Gaussian doublet in the S region, indicative of uniform Au–S bonding. The presence of two Gaussian doublets, needed for the disulfide-modified oligonucleotides, suggests that sulfur is present in both physi- and chemisorbed states. Voltammetry and interfacial capacitance data of the thiol-linked 25-mer oligonucleotides result in strong reductive desorption peaks around −700 mV (vs. SCE). The voltammetric peak area accords with high HS-ss25-mer coverage, compatible with adsorption in an upright or tilted position on the strongly negatively charged electrode surface. In situ STM of DMT-SS-$(AT)_{10}$ and A_{10}-S-S-T_{10} shows, finally, that the coverage of the former is by far the lowest, probably because the bulky DMT group blocks favorable lateral interactions between the adsorbate molecules.

The study has combined XPS, state-of-the-art physical electrochemistry including voltammetry, interfacial capacitance, and in situ STM directly in aqueous biological media. Polycrystalline and well-characterized single-crystal and atomically planar Au(111) surfaces have constituted the micro-environments. The study has shown that this comprehensive approach discloses novel detail in the structure and dynamics of short oligonucleotide adsorption, with resolution at the single-molecule level.

Acknowledgements Financial support by the FREJA programme and The Danish Technical Science Research Council is acknowledged.

References

1. Service RF (1998) Science 282:396
2. Southern E, Mir K, Shchepinov M (1999) Nat Genet 21:5
3. Fritz J, Baller MK, Lang HP, Rothuizen H, Vettiger P, Meyer E, Güntherodt HJ, Gerber C, Gimzewski JK (2000) Science 288:316
4. Bashir R (2001) Superlattices Microstruct 29:1
5. O'Kelley S, Barton JK, Jackson NM, McPherson LD, Potter AB, Spain EM, Allen MJ, Hill MG (1998) Langmuir 14:6781
6. O'Kelley S, Jackson NM, Hill MG, Barton JK (1999) Angew Chem Int Ed 38:941
7. Giese B (2000) Acc Chem Res 33:631
8. Jortner J, Bixon M, Langenbacher T, Michel-Beyerle ME (1998) Proc Natl Acad Sci USA 95:12759
9. Bixon M, Jortner J (2000) J Phys Chem B 104:3906
10. Bixon M, Jortner J (2002) Chem Phys 281:393
11. Davis WB, Hess S, Naydenova I, Haselsberger R, Ogrodnik A, Newton MD, Michel-Beyerle ME (2002) J Am Chem Soc 124:2422
12. Berlin YA, Burin AL, Ratner MA (2000) Superlattices Microstruct 28:241
13. Wooster R, Weber BL (2003) N Engl J Med 348:2339
14. Zhang J Grubb M, Hansen AG, Kuznetsov AM, Boisen A, Wackerbarth H, Ulstrup J (2003) J Phys C 15:1873
15. Clavilier J, Faure R, Guinet G, Durand R (1980) J Electroanal Chem 107:205
16. Hamelin A (1996) J Electroanal Chem 411:1
17. O'Brien JC, Jones VW, Porter MD (2000) Anal Chem 72:703
18. Bourg MC, Badia A, Lennox RB (2000) J Phys Chem B 104:6562
19. Chi Q, Zhang J, Friis EP, Andersen JET, Ulstrup J (1999) Electrochem Commun 1:91
20. Chi Q, Zhang J, Nielsen JU, Friis EP, Chorkendorff I, Canters GW, Andersen JET, Ulstrup J (2000) J Am Chem Soc 122:4047
21. Hansen AG (2002) PhD thesis. Technical University of Denmark
22. Long YT, Li CZ, Kraatz HB, Lee JS (2003) Biophys J 84:3218
23. Ishida T, Yamamoto S, Mizutani W, Motomatsu M, Tokumoto H, Hokari H, Azehara H, Fujihira M (1997) Langmuir 13:3261
24. Hinnen C, Rousseau A, Parsons R (1981) J Electroanal Chem 125:193
25. Webb JW, Janik B, Elving PJ (1973) J Am Chem Soc 95:8495
26. Haiss W, Roelfs B, Port SN, Bunge E, Baumgärtel H, Nichols RJ (1998) J Electroanal Chem 454:107
27. Roelfs B, Port SN, Bunge E, Schröter C, Solomun T, Meyer H, Nichols RJ, Baumgärtel H (1997) J Phys Chem B 101:754
28. Tao NT, DeRose JA, Lindsay SM (1993) J. Phys Chem. 97:910
29. Hasoň S, Vetterl V (2002) Bioelectrochemistry 56:43
30. Yang DF, Wilde CP, Morin M (1996) Langmuir 12:6570
31. Yang DF, Wilde CP, Morin M (1997) Langmuir 13:243
32. Esplandiu MJ, Hagenström H, Kolb DM (2001) Langmuir 17:828
33. Zhang RY, Pang DW, Zhang ZL, Yan JW, Yao JL, Tian ZQ, Mao BW, Sun SG (2002) J Phys Chem B 106:11233
34. Wackerbarth H, Grubb M, Zhang J, Hansen AG, Ulstrup J (2003) Angew Chem Int Ed (in press)
35. Herne TM, Tarlov MJ (1997) J Am Chem Soc 119:8916